A small RNA controls bacterial resistance to gentamicin during iron starvation

Short title: RyhB promotes resistance to gentamicin

Sylvia Chareyre[1], Frédéric Barras[1, 2] and Pierre Mandin[1]*

[1] : Aix Marseille Univ – CNRS, Laboratoire de Chimie Bactérienne, Institut de Microbiologie de la Méditéranée, 31 chemin Joseph Aiguier, 13009 Marseille, France

[2] : Departement de Microbiologie, Institut Pasteur, 28 rue du Dr Roux, 75015 Paris, France

* : to whom correspondence should be addressed

pmandin@imm.cnrs.fr

Keywords: antibiotics resistance, ncRNAs, RyhB, Fe-S clusters, respiratory complexes

ABSTRACT

Phenotypic resistance describes a bacterial population that becomes transiently resistant to an antibiotic without requiring a genetic change. We here investigated the role of the small regulatory RNA (sRNA) RyhB, a key contributor to iron homeostasis, in the phenotypic resistance of *Escherichia coli* to various classes of antibiotics. We found that RyhB induces resistance to gentamicin, an aminoglycoside that targets the ribosome, when iron is scarce. RyhB induced resistance is due to the inhibition of respiratory complexes Nuo and Sdh activities**.** These complexes, which contain numerous Fe-S clusters, are crucial for generating a proton motive force (pmf) that allows gentamicin uptake. RyhB directly represses the expression of *nuo* and *sdh* operons by binding to their mRNAs, thereby inhibiting their translation. Indirectly, RyhB also inhibits the maturation of Nuo and Sdh by repressing synthesis of the Isc Fe-S biogenesis machinery. Notably, our study identifies *nuo* as a new direct RyhB target and shows that respiratory complexes activity levels are predictive of the bacterial sensitivity to gentamicin. Altogether, these results unveil a new role for RyhB in the adaptation to antibiotic stress, an unprecedented consequences of its role in iron starvation stress response.

37

38 ## AUTHOR'S SUMMARY

39 Understanding the mechanisms at work behind bacterial antibiotic resistance has
40 become a major health issue in the face of the antibiotics crisis. Here, we show that
41 RyhB, a bacterial small regulatory RNA, induces resistance of *Escherichia coli* to the
42 antibiotic gentamicin when iron is scarce, an environmental situation prevalent during
43 host-pathogen interactions. This resistance is due to RyhB repression of the
44 synthesis and post-translational maturation of the respiratory complexes Nuo and
45 Sdh. These complexes are crucial in producing the proton motive force that allows
46 uptake of the antibiotics in the cell. Altogether, these data point out to a major role for
47 RyhB in escaping antibacterial action.

Introduction

The emergence and spread of bacterial multi-resistance to antibiotics has become a major health issue in the last decades, urging for the development of new anti-bacterial molecules and for a better understanding of the molecular mechanisms at work behind bacterial resistance (1,2). While acquired resistance mechanisms (acquisition of genes or mutations that confer resistance) have long been the main focus of attention, less is known about “phenotypic” resistance, which is the process in which a bacterial population becomes transiently resistant to an antibiotic without requiring a genetic change (3–5). For instance, this kind of resistance has been associated with specific processes such as stationary growth phase, persistence and metabolic changes, reinforcing the idea that the environment encountered by the pathogen is a key determinant for antibiotic susceptibility (6).

Change in utilization of iron-sulfur (Fe-S) cluster biogenesis machineries in *Escherichia coli* gives a striking example of phenotypic resistance (7). Fe-S clusters are ubiquitous and ancient cofactors used in a plethora of biological processes, such as metabolism and respiration (8,9). In *E. coli*, Fe–S clusters are formed and brought to target proteins thanks to two dedicated biogenesis systems: the so called “housekeeping” Isc machinery, which homologs are found in mitochondria of eukaryotic organisms, and the stress-responsive Suf system, in which homologs are found in chloroplasts of plants (10,11). These systems are responsible for the maturation of more than 150 Fe-S cluster containing proteins in *E. coli*, notably numerous proteins contained in the main respiratory complexes I (Nuo) and II (Sdh) (12–14). Strikingly, it was shown that impairment of the *E. coli* Isc machinery

enhances resistance to aminoglycosides, a well-known class of antibiotics that target the ribosome (7). This resistance is due to a deficiency in the maturation of the respiratory complexes in *isc* mutants, which in turn leads to a decrease in the proton motive force (pmf) that is essential for aminoglycosides uptake (15). Incidentally, it was deduced from these results that the Suf machinery is unable to maturate efficiently the Fe-S cluster containing proteins of the respiratory complexes, although the molecular reason for this still remains unclear. Overall this study predicted that an environmental signal that induces the switch from Isc to Suf should induce a transient resistance to aminoglycosides.

Iron starvation is one signal that decreases the expression of the isc operon encoding the Isc pathway. The small RNA RyhB mediates this regulation.(16). RyhB is one of the most studied sRNAs to date in *E. coli* (17–19). RyhB is regulated by Fur, the main regulator of Fe-homeostasis in many bacteria and is expressed during iron starvation (20,21). When iron becomes limiting in the medium, RyhB base-pairs and represses the translation of more than 100 mRNA targets that encode for non-essential iron-utilizing proteins, thus engaging an “iron sparing” response and redirecting iron consumption in the cell (19). RyhB was shown to participate in the Isc to Suf transition during iron starvation by binding to the *iscRSUA* mRNA (16). In this way, it induces the degradation of the 3’ part of the mRNA that contains *iscSUA*, encoding the Isc machinery, while the 5’ part that encodes *iscR* remains stable. IscR is the major regulator of Fe-S clusters homeostasis and is itself a Fe-S cluster protein maturated by Isc (22). Accumulation of IscR in its apo-form has been shown to induce the *suf* operon (23). By its differential regulation of the *isc* operon, RyhB thus

leads to the accumulation of apo-IscR that will turn on the expression of the alternative Suf system during iron starvation.

Iron homeostasis in particular has been shown to modify the sensitivity of bacteria to a number of antibiotics, although the molecular basis behind this is not always clear (24). Here we asked if the sRNA RyhB could participate in phenotypic resistance to various antibiotics during iron starvation. We found that RyhB is necessary to induce aminoglycoside resistance in low iron conditions. By further investigating the mechanism by which RyhB controls this phenotypic resistance, we show that RyhB controls entry of aminoglycosides in the cell by acting at both the synthesis and the maturation levels of the two pmf-producing respiratory complexes Nuo and Sdh.

Results

RyhB is involved in resistance to the aminoglycoside gentamicin

We first investigated the possible role of RyhB in resistance against different class of antibiotics during iron starvation. To do so, we performed antibiotic killing assays by growing wild type (WT) and *ryhB* mutant cells in LB medium starved or not for iron using 250 μM of dipyridyl (DIP), a strong iron chelator. We chose this concentration of DIP because it is known to induce RyhB and we checked that it did not affect the growth of the cells (25,26). Antibiotics were added when cells reached early exponential phase (OD_{600}= 0.2) and the number of survivors was determined by counting the number of colony forming units (c.f.u) after 3 hours of incubation. Four different major classes of antibiotics were tested: aminoglycosides (gentamicin), β-lactams (ampicillin), fluoroquinolones (norfloxacin), and tetracycline.

As expected, both WT and *ryhB* mutant cells were sensitive to the presence of all classes of antibiotics when grown in medium not starved for iron (Fig. 1A to D, left panels). Iron chelation did not protect cells against tetracycline (Fig. 1C). In contrast, adding DIP to the medium induced a protective effect on the WT and *ryhB* mutant strains for ampicillin and norfloxacin (Fig. 1A-B). The protective effect of iron deprivation for these antibiotics has already been observed and its underlying cause has been greatly debated (7,24,27,28). As cells were protected independently of *ryhB,* we did not pursue these antibiotics further. In contrast, WT cells were protected against gentamicin when DIP was added to the medium, but this protection effect was lost when cells were mutated for *ryhB*. This result thus suggested that RyhB is

129 involved in the protection of bacterial cells against aminoglycosides during iron
130 starvation (Fig. 1D).

131 To further investigate this phenotype, we performed gentamicin kinetic killing
132 assays by growing WT or *ryhB* mutant cells in presence of DIP and counting the
133 number of surviving bacteria at different time intervals after addition of the antibiotic.
134 In this experiment, both the WT and *ΔryhB* strains showed the same profile when
135 grown in LB (Fig. 1E). In both cases, the majority of the cells were rapidly killed after
136 1 h 30 min of incubation with gentamicin (5 logs of killing). Again, addition of DIP to
137 the medium had a ≈ 4 log protective effect against gentamicin on WT cells as early as
138 1 h 30 min post addition of the antibiotic. Cells then remained mainly resistant to
139 gentamicin during the course of the experiment. In contrast, the *ryhB* mutant
140 gradually became as sensitive as cells grown in the absence of DIP (see 4 h 30 min
141 time point), although killing kinetics were slightly slower than in presence of iron.
142 Finally, to better characterize the effect of RyhB on gentamycin efficacy during iron
143 starvation, we performed minimum inhibitory concentration assays (MIC) by growing
144 WT and *ryhB* mutants in presence of increasing concentration of gentamicin, with or
145 without DIP. Growing cells in presence of DIP almost doubled the MIC of the WT cells
146 (from 6 *μ*g/mL in LB to 10 *μ*g/mL in presence of DIP) (Figure S1). In sharp contrast,
147 the protective effect allowed by DIP was completely lost in the *ryhB* mutant.
148 Altogether, these results indicated that RyhB is needed for the phenotypic resistance
149 of *E. coli* to gentamicin in low iron condition.
150
151 **The RyhB induced resistance to gentamicin is dependent on Nuo and Sdh**

Uptake of gentamicin has been shown to be a crucial step in the phenotypic resistance against this aminoglycoside (7). Entry of aminoglycosides is dependent on the proton motive force (pmf) mainly produced directly by respiratory complex I and indirectly by the respiratory complex II, respectively encoded by the *nuo* and *sdh* operon (12,15,29). Thus, one hypothesis was that RyhB induced resistance was due to an inhibitory effect on the activity of these two complexes that would block entry of gentamicin in the cell.

To test this hypothesis we repeated the previous killing assays in a strain deleted for both respiratory complexes (*Δnuo Δsdh*). As expected, this mutant was resistant to gentamicin (Fig. 2, left panel) (7). Adding DIP to the medium somewhat increased by 1 log the survival of the *nuo sdh* mutant, suggesting that pmf might be even more decreased in these conditions. Nevertheless, deleting *ryhB* from this strain did not increase its sensitivity to gentamicin during iron starvation (Fig. 2, right panel) indicating that the phenotype induced by RyhB was dependent on *nuo* and *sdh*.

We further assessed the implication of each of the respiratory complexes by testing the sensitivity of the *Δnuo* and *Δsdh* simple mutants, deleted or not for *ryhB* (Fig. S2). The *nuo* simple mutant was almost completely resistant to gentamicin in presence of DIP, whether *ryhB* was present or not. In contrast, the *sdh* simple mutant became somewhat more sensitive (1 log) when *ryhB* was deleted from the chromosome. We conclude from these results that while both complexes are needed for full sensitivity of *ryhB* mutants to gentamicin, Nuo seems to be slightly more important than Sdh.

RyhB represses the activity of the respiratory complexes

These previous results suggested that RyhB inhibits the activity of both respiratory complexes during iron starvation. To test this, we measured Nuo and Sdh specific enzymatic activities in WT and *ryhB* mutant strains grown in presence or absence of the iron chelator DIP in the growth medium. Nuo activity was decreased when the WT strain was grown in LB medium depleted for iron (about 4-fold) (Fig. 3A). In contrast, deleting *ryhB* from the chromosome restored 75% of Nuo activity in presence of DIP. The same pattern was also observed for Sdh activity (Fig. 3B). Altogether, these results confirm that RyhB represses the activities of both Nuo and Sdh complexes in medium deprived for iron.

RyhB represses *nuo* and *sdh* expression

RyhB inhibition of Sdh and Nuo activities may be due to the repression of the synthesis and / or of the maturation of the complexes. Expression of *sdh* has already been shown to be repressed by RyhB (20,30). In contrast, although pointed out in global approaches, RyhB regulation of *nuo* genes expression still awaited investigation (17,31–33).

Using the RNA-fold software (http://unafold.rna.albany.edu), we could predict a base-pairing in between RyhB and the 5' un-translated region of the first gene of operon, *nuoA* (34). This base-pairing involves 21 nucleotides (nt) of RyhB and includes the ribosome-binding site (RBS) and the start codon of *nuoA* (Fig. 4A). Overexpression of *ryhB* on a plasmid decreased the activity of a P_{BAD}-*nuoA-lacZ* fusion of about 4-fold, as compared to cells transformed with an empty vector (Fig. 4B). In addition, the P_{BAD}-*nuoA-lacZ* activity was decreased by 2-fold when WT

cells were treated with DIP. This was in sharp contrast with the isogenic *ryhB* mutant strain for which activity remained the same in presence or absence of DIP (Fig. 4C).

We then tested the biological relevance of the predicted base-pairing by introducing point mutations in the P_{BAD}-*nuoA-lacZ* chromosomal fusion, giving rise to the *nuoA*$_{mut}$-*lacZ* fusion (G86C and C87G; Fig. 4A). In contrast to the WT *nuoA-lacZ* fusion, RyhB overexpression was no longer able to repress activity of the *nuoA*$_{mut}$ fusion (Fig. 4D). We then introduced compensatory mutations in the pRyhB plasmid that should restore base-pairing to the mutated, but not to the WT, *nuo-lacZ* fusion, giving rise to pRyhB$_{mut}$. As seen in figure 4D, overexpression of RyhB$_{mut}$ failed to fully repress the WT *nuo-lacZ* fusion, but was able to repress *nuoA*$_{mut}$-*lacZ* fusion. Altogether these results show that RyhB represses *nuo* expression by base-pairing on the mRNA upstream *nuoA*.

We then evaluated the effect of this repression on protein levels by performing Western blot analyses against NuoG, a protein of the complex. Strikingly, NuoG protein levels decreased steeply, about 3-fold, when the WT strain was grown in presence of DIP (Fig. 4E). This phenotype was suppressed in the *ryhB* mutant, confirming the *in vivo* inhibition of Nuo synthesis by RyhB.

As a control and to compare *sdh* regulation to *nuo*, we performed a series of similar tests on an *sdhC-lacZ* fusion. We saw that RyhB overexpression repressed the expression of the fusion by more than 10 fold (Fig. S3A). In addition, the WT fusion was also strongly inhibited when cells were grown in presence of DIP but not when *ryhB* was deleted from the chromosome (Fig. S3B). Identical conclusions were reached from analyzing SdhB protein levels by performing Western blots (Fig. S3C). These experiments thus confirm the regulation of *sdh* by RyhB in our conditions.

223

224 **RyhB inhibits Nuo and Sdh maturation by repressing *iscSUA***

225 Biogenesis of Fe-S clusters by the Isc machinery has been shown to be key
226 for full Nuo and Sdh activity and their associated pmf production. The *iscSUA* mRNA
227 is a known RyhB target (16). Therefore, we asked if reducing levels of the Isc
228 machinery synthesis following RyhB inhibition would be sufficiently important such as
229 it would bear consequences on maturation of Nuo and Sdh.

230 To do so, we measured Nuo and Sdh specific activities in strains deleted for
231 *suf* or for *isc* with or without *ryhB* (Fig. 5). In agreement with the literature, Nuo
232 activity was decreased more than 5 fold in an *isc* mutant where the Suf machinery
233 alone is responsible for Fe-S biogenesis (Fig. 5A). Activities of the *isc* mutant
234 remained low in iron-deprived conditions, even when RyhB-mediated repression of
235 Nuo and Sdh respiratory complexes synthesis was alleviated by deleting *ryhB*. Nuo
236 activity of the *Δsuf* strain was comparable to that of the WT and DIP treatment
237 inflicted the same drop in activity. Strikingly however, further deleting *ryhB* in the *suf*
238 mutant almost completely restored Nuo activity when cells were grown in low iron
239 condition. Thus, we concluded that repression of *iscSUA* and *nuo* by RyhB is
240 sufficient to almost abolish Nuo activity. Moreover, these data strongly suggest that
241 Isc is the only system that allows Fe-S clusters maturation of Nuo complex,
242 regardless of the iron concentration in the medium.

243 The situation was slightly different for Sdh. Deleting *isc* severely affected
244 activity of Sdh in presence or absence of iron. In sharp contrast to Nuo however,
245 activity of Sdh was not restored when *ryhB* was deleted from the *suf* mutant (Fig. 5B).
246 Further deleting *ryhB* from this strain marginally restored Sdh activity, indicating that

Suf can at least partially maturate Sdh proteins that are produced in absence of *ryhB.* These results thus suggest that Isc cannot ensure maturation of Sdh in low iron conditions.

RyhB induces gentamicin resistance by repressing *isc*, *nuo* and *sdh* expression

In order to better appraise the role of Fe-S clusters maturation inhibition by RyhB in the resistance to gentamicin, we performed sensitivity assays in strains containing only one of the two Fe-S biogenesis machineries. As previously shown, the *isc* mutant was fully resistant to gentamicin in LB (Fig. 6A) (7). This phenotype remained unchanged when DIP was added to the medium, whether RyhB was present or not (Fig. 6A), thus showing that the slight Sdh activity observed in these conditions (Fig. 5) is not sufficient to render the cells sensitive to gentamicin. In sharp contrast, introducing a *ryhB* mutation restored sensitivity of a *suf* mutant strain when grown in presence of DIP (Fig. 6B), which is in agreement with the restoration of Nuo activity in this strain under these conditions.

As Nuo and Sdh activities are determinants for gentamicin sensitivity, we investigated if we could correlate both the levels of complexes enzymatic activity with that of resistance to gentamicin. Strikingly, there was an almost linear correlation between Nuo or Sdh activities of each strain and its sensitivity to gentamicin (Fig. S4 A and B). For instance, strains displaying the lowest Nuo activities were the most resistant to gentamicin, and vice versa.

Taken together, the ensemble of these results show that the maturation of Nuo and Sdh by Isc is essential for pmf production and that RyhB phenotypic resistance to

271 gentamicin is due to both the direct inhibition of the expression of *nuo* and *sdh*, but

272 also indirectly to the inhibition of Nuo maturation by Isc.

273

Discussion

Phenotypic resistance can take place when environmental conditions change the metabolic state of the cell. Adaptative molecular responses modify cellular physiology, which induce a transient resistance state. Here, we show that the sRNA RyhB is a major contributor of *E. coli* phenotypic resistance to gentamicin in iron limiting conditions. Aminoglycosides uptake depends upon the activity of respiratory complexes I (Nuo) and II (Sdh) that produce pmf, directly and indirectly, respectively. RyhB acts negatively on both respiratory complexes, directly at the level of their synthesis and indirectly at the level of their maturation (i.e. acquisition of Fe-S clusters) (Fig. 7). Our model strengthens the role of the pmf-producing respiratory complexes in entry of aminoglycosides. Fe-S biogenesis maturation of the complexes was earlier pointed out as the main factor for resistance (7). By identifying here that the *nuo* mRNA is targeted by RyhB in addition to *sdh*, we show that synthesis of the respiratory complexes is also key in this process.

As early as 2005, the *nuo* mRNA was suspected to be a target of RyhB as the operon was down-regulated when the sRNA was over-expressed, (17). The *nuo* mRNA was also more recently found associated with Hfq and RyhB in a global study of sRNA-mRNA interactions (33). We here could predict and confirm a direct base-pairing of RyhB to the *nuo* mRNA at the level of the UTR of *nuoA,* the first gene of the operon. This base-pairing occurs close to the ribosome binding site of *nuoA*, which strongly suggests that RyhB represses expression of *nuo* in a “classical” way, *i.e.* by occluding binding of the ribosome, leading to the degradation of the mRNA (35). The *nuo* mRNA is very long (about 15 kb) and comprises 14 genes, which makes it one of

298 the longest mRNAs regulated by a sRNA to our knowledge. Importantly, in addition to
299 the effects seen on *nuoA* by our beta-galactosidase assays (Fig. 4), we could also
300 observe by Western blots RyhB repression on NuoG level (Fig. 4E), whose gene lies
301 more than 5 kb away from the base-pairing site. It will thus be interesting to
302 investigate how far downstream repression inhibits expression of the *nuo* operon.

303 Respiratory complexes are high iron consumers, with a total of 12 Fe-S
304 clusters for Nuo and Sdh in *E. coli*. Thus, their repression by RyhB is in line with its
305 role in installing an iron sparing response when iron becomes scarce (17,19). Before
306 our results, one could have imagined that RyhB represses Nuo and Sdh expression
307 in order to limit accumulation of inactive apo-complexes in iron scarce conditions.
308 However, both protein levels and activity of Nuo are restored in a *ryhB* mutant in iron-
309 deprived medium indicating that maturation of respiratory complex I is possible under
310 these conditions. These results strongly suggest that RyhB inhibits synthesis of Nuo
311 Sdh not because they cannot be matured, but rather to preclude respiratory
312 complexes to divert iron from other essential processes.

313 By repressing the *iscSUA* mRNA expression, RyhB also inhibits indirectly the
314 maturation of Nuo (Fig. 3A and Fig. 5A). In contrast, maturation of Sdh was only
315 partially restored in the *ryhB* mutant in presence of DIP (Fig. 3B) and, perhaps more
316 surprisingly, this activity did not seem to be dependent on Isc but rather on Suf (Fig.
317 5B). More investigation is needed to understand the molecular basis for the
318 difference in between Isc and Suf substrates preference. In any case, our results also
319 clearly show that Nuo activity is more important than that of Sdh in installing a
320 phenotypic resistance to gentamicin (Fig. S2). This may relate to pmf production by
321 Nuo and Sdh. Indeed, Nuo, but not Sdh, directly translocates 4 protons across the

membrane, while both indirectly contribute to pmf production by passing electons to cytochrome oxydase (12,36).

The inhibition of respiratory complexes activity suggests that RyhB controls a complete metabolic shift during iron starvation, likely from respiration to fermentation. Although much needs to be done to assess this hypothesis, our recent survey indicates that a significant number of genes encoding Fe—S dependent enzyme of the TCA cycle are under the negative control of RyhB (19). Whether their maturation is also under RyhB influence via its control of the Isc system is an exciting issue to address.

Our study puts RyhB on the focus among a growing number of sRNAs that have been directly or indirectly linked to antibiotic resistance (36–38). However, in most of these cases phenotypes were derived from overexpression of the sRNAs and not relevant to physiological conditions. For instance, 17 out of 26 *E. coli* sRNAs that were assessed in a systematic manner against a variety of antibacterial effectors were shown to affect sensitivity to antibiotics when overexpressed, but few showed any phenotype when mutated (39).

A most spectacular case is represented by the role RyhB could play in the bacterial persistence of uropathogenic *E. coli* to different classes of antibiotics, among which included gentamicin (40). Persistence is a phenomenon in which a fraction of the bacterial population enters a metabolically inactive state that enables it to survive exposure to bactericidal antibiotics (41). Interestingly, in this study it was proposed that *ryhB* mutants would induce less persister cells because they display increased ATP levels and altered NAD^+ / NADH ratios. In the light of our results, we believe these effects are explained by the fact that *ryhB* mutants probably display

346 higher levels of Nuo, Sdh and Isc and therefore are more metabolically active, but
347 also more prone to uptake the antibiotic. It is noteworthy that these experiments were
348 conducted in rich medium not devoid for iron, and after long treatment with antibiotics
349 (four days), which may explain low induction of RyhB in only a small percentage of
350 bacterial cells that would then be able to resist antibiotics treatment in a persister-like
351 manner.

352 RyhB homologs and paralogs are found in multiple other bacterial species,
353 which suggests that many bacteria outside of *E. coli* may share the resistance
354 mechanism that we describe here (19,42–44). In particular, other pathogenic bacteria
355 such as *Yersinia, Shigella* or *Salmonella* possess not only RyhB homologs, but also
356 the Isc and Suf system and rely on Nuo and Sdh for respiration on oxygen (45,46).
357 RyhB has also been implicated in promoting sensitivity to colicin IA, which is not an
358 antibiotic in a narrow sense, but a bacteriocin secreted by other species to
359 outcompete bacteria sharing the same niches (47). In addition, RyhB has been
360 shown to be involved in the virulence of *Shigella dysenteriae* by repressing the major
361 virulence regulator *virB*, and the sRNA may be associated with the virulence of
362 *Yersinia pestis,* as the expression of its two RyhB homologs (RyhB1 and RyhB2)
363 increases in the lung of infected mice (43,48). Altogether, these data point out for a
364 major role for RyhB in escaping antibacterial action.

Materials and methods

Strains and culture

All strains used in this study are derivatives of *E. coli* MG1655 and are listed in Table S1. Strains were grown in LB broth (Difco), containing various concentrations of 2,2'-dipyridyl (DIP) (Sigma) when stated. Transductions with P1 phage were used for moving marked mutation as described previously in (49). The plac and pRyhB plasmids used in this study are described and have been transformed as previously described in (50). All oligonucleotides used are listed in Table S2.

Antibiotic sensitivity experiments

Starting from overnight cultures in LB, strains were diluted 1/100 time in fresh medium containing or not DIP and grown aerobically at 37 °C with shaking until $OD_{600} \approx 0.2$. At this point, antibiotics were added to the cells (gentamicin: 5 µg / mL; ampicillin: 5 µg / mL; tetracycline: 5 µg / mL and norfloxacin: 25 ng / mL). After 3 h cells were taken, diluted in PBS buffer and spotted on LB agar plates and incubated at 37 °C for 16 h. Cell survival was determined by counting the number of colony-forming units per mL (c.f.u. / mL). The absolute c.f.u at time-point 0 was of $\approx 5 \times 10^7$ cells / mL in all experiments.

Minimum inhibitory concentration (MIC) determination

The MIC were determined as previously described (51). Briefly, each antibiotic containing-well of a 96-well micro-titer plate was inoculated with 100 µL of a fresh LB bacterial inoculum of 2×10^5 c.f.u / mL. The plate was incubated at 37°C for 18 h

under aerobic conditions. OD_{600} for each well was then determined by measuring the absorbance on a Tecan infinite 200. MIC was defined as the lowest drug concentration that exhibited complete inhibition of microbial growth.

Fusions construction

The P_{BAD}-*nuoA-lacZ* and P_{BAD}-*sdhC-lacZ* fusions were constructed and recombined in PM1205 strain, as previously described (25). Briefly, sequences corresponding to *nuo or sdh* genes starting from its +1 transcriptional start up to 30 nucleotides downstream of the ATG codon were amplified using oligonucleotides P_{BAD}-nuoA-F or P_{BAD}-sdhC-F, and lacZ-nuoA-R or lacZ-sdhC-R, respectively. PCR amplifications were carried out using the EconoTaq DNA polymerase from Lucigen. The purified PCR products were then electroporated into strain PM1205 for recombination at the *lacZ* site. Recombinants carrying the desired fusions (SC005 and SC009) were selected on LB plates devoid of NaCl and containing 5 % sucrose, 0,2 % arabinose and 40 µg / mL X-Gal (5-bromo-4-chloro-3-indolyl-D-galactopyranoside). Blue colonies were chosen, and the resulting fusions were sequenced using oligonucleotides lacI-F and Deep-lac.

Overlap PCR was used to introduce point mutation in the fusion. The two PCR products corresponding to the sequence upstream and downstream of the desired mutation were amplified by PCR with oligonucleotides nuoAmut-F and Deep-lac, and LacI-F and nuoAmut-R containing the desired mutation and using genomic DNA from the SC005 strain as a template. The two PCR products were then joined by an

412 overlap PCR using oligonucleotides lacI-F and Deep-lac. The resulting PCR products
413 were purified, electroporated in strain PM1205 and sequenced as described above.
414 For point mutations in the pRyhB plasmid, the pRyhB plasmid was first purified
415 from a WT (dam$^+$) *E. coli* strain, and then amplified by PCR with oligonucleotides
416 RyhBmut-F and RyhBmut-R, containing the desired mutation. The native plasmid was
417 eliminated from the resulting PCR product by Dpn1 enzyme digestion for 1 h at 37 °C.
418 Plasmids containing the desired mutation were then purified and transformed in
419 SC005 and SC0026 strains.
420
421 **β-galactosidase experiments**
422 Overnight cultures of different strains were diluted 1/100 times in fresh medium
423 in culture flasks containing ampicillin and IPTG (isopropyl ß-D-
424 1thiogalactopyranoside) or DIP when indicated. After ≈ 7 hours of growth 100 µL of
425 cultures were dispatched in 96 wells microtiter plates (triplicates for each conditions).
426 Absorbance at 600 nm was measured in a microtiter plate reader (Tecan infinite 200
427 ®). Then, 50 µL of permeabilization buffer were added in each well (100 mM Tris HCl
428 pH 7,8; 32 mM Na_2HPO_4; 8 mM EDTA; 40 mM Triton; H_2O milli Q) and the microtiter
429 plate was incubated for 10 minutes at room temperature. O-Nitrophenyl-β-D-
430 galactopyranoside (ONPG) was added to the solution and appearance of its
431 degradation product was immediately determined by measuring the absorbance at
432 420 nm on a Tecan infinite 200 during 30 minutes. The specific activities were
433 calculated by measuring the Vmax of the OD_{420} appearance divided by the OD_{600}.
434 Values were then multiplied by 100000, a coefficient that was chosen empirically to
435 approximate Miller units.

436

437 **Nuo and Sdh enzymatic activities**

438 The Nuo and Sdh enzymatic activities were determined as previously described
439 (52,53). Briefly, overnight cultures of the strains of interest were diluted 1/100 times in
440 fresh LB medium containing or not 250 µM of DIP and grown at 37 °C with shaking
441 until they reached $OD_{600} \approx 0.6$. Cultures were pelleted by centrifugation (11 000 G,
442 10 min at 4 °C) and washed in phosphate buffer (50 mM pH 7,5). Cells were then
443 lysed at the French press and 100 μL were immediately frozen in liquid nitrogen
444 before determining Nuo activity. Nuo enzymatic activity was determined at 30 °C by
445 monitoring the disappearance of the specific Deamino-NADH (DNADH) substrate at
446 340 nm every 5 s during 10 min at 30 °C in a spectrophotometer.

447 For Sdh activity determination, lysate samples from French press were pellet
448 by centrifugation (11 000 G, 10 min at 4 °C) and the supernatant was used for
449 membrane fraction preparation by ultracentrifugation at 45 000 G at 4 °C during two
450 hours. Pellets were then resuspended in phosphate buffer and kept in liquid nitrogen
451 for later Sdh activity measurements. The enzyme was first activated by incubation in
452 50 mM Tris-HCl (pH 7.5), 4 mM succinate, 1 mM KCN for 30 min at 30 °C. The
453 enzymatic activity was measured in the membrane fraction by monitoring Phenazine
454 EthoSulfate (PES)-coupled reduction of dichlorophenol indophenol (DCPIP) at
455 600 nm, in a reaction containing 50 mM Tris-HCl (pH 7.5), 4 mM succinate, 1
456 mM KCN, 400 µM PES and 50 µM DCPIP.

457 The specific activities were calculated by measuring the Vmax divided by the
458 protein concentration in total extracts evaluated by absorbance at 280 nm.

459

460 **Quantification of Nuo and Sdh protein levels by Western blot analyses**

461 Total extracts and membranes preparation prepared for Nuo and Sdh activities were
462 used for quantification of Nuo and Sdh protein levels, respectively. Total protein
463 levels were determined by measuring absorbance at 280 nm on a
464 spectrophotometer. Same amount of total protein level were migrated on poly-
465 acrylamide gels Tris-gly Sodium Dodecyl Sulfate (Novex 4-20 % Tris-Glycine Mini
466 Gels) then, transferred on nitrocellulose membrane using Pierce G2 Fast Blotter
467 (25 V, 1,3 mA, 7 min). Protein level were detected by incubating the membrane with
468 α-NuoG or α-SdhB (1/1000) antibodies from rabbit and then by an α-rabbit antibody
469 (1/1000) coupled with Hrp peroxidase. Signals were detected by chemiluminescence
470 with Pierce ECL Western blotting system on an ImageQuant LAS 4000 camera.
471 Quantification of protein levels was determined by measuring the specific signal
472 intensity of the bands corresponding to Nuo and Sdh proteins with the ImageJ
473 software. Intensities were normalized using an unspecific band detected by the same
474 antibody.

475 # Acknowledgements

476

477 We would like to thank A. Battesti for precious help with strain constructions and A.
478 Huguenot for critical guidance with enzymatic activities assays. P.M., F.B. and S.C.
479 work was funded by the Centre National de la Recherche Scientifique (CNRS) and
480 Aix Marseille Université (AMU). S.C. is a recipient of a Fondation pour la Recherche
481 Médicale grant (FDT20170436820).

References

1. Woolhouse M, Waugh C, Perry MR, Nair H. Global disease burden due to antibiotic resistance - state of the evidence. J Glob Health. 2016 Jun;6(1):010306.

2. Laxminarayan R, Matsoso P, Pant S, Brower C, Røttingen J-A, Klugman K, et al. Access to effective antimicrobials: a worldwide challenge. Lancet Lond Engl. 2016 Jan 9;387(10014):168–75.

3. van Hoek AHAM, Mevius D, Guerra B, Mullany P, Roberts AP, Aarts HJM. Acquired Antibiotic Resistance Genes: An Overview. Front Microbiol [Internet]. 2011 Sep 28;2. Available from: https://www.ncbi.nlm.nih.gov/pmc/articles/PMC3202223/

4. Munita JM, Arias CA. Mechanisms of Antibiotic Resistance. Microbiol Spectr [Internet]. 2016 Apr;4(2). Available from: https://www.ncbi.nlm.nih.gov/pmc/articles/PMC4888801/

5. Corona F, Martinez JL. Phenotypic Resistance to Antibiotics. Antibiotics. 2013 Apr 18;2(2):237–55.

6. Poole K. Bacterial stress responses as determinants of antimicrobial resistance. J Antimicrob Chemother. 2012 Sep;67(9):2069–89.

7. Ezraty B, Vergnes A, Banzhaf M, Duverger Y, Huguenot A, Brochado AR, et al. Fe-S cluster biosynthesis controls uptake of aminoglycosides in a ROS-less death pathway. Science. 2013 Jun 28;340(6140):1583–7.

8. Fontecave M. Iron-sulfur clusters: ever-expanding roles. Nat Chem Biol. 2006 Apr;2(4):171–4.

503 9. Kiley PJ, Beinert H. The role of Fe-S proteins in sensing and regulation in bacteria. Curr
504 Opin Microbiol. 2003 Apr;6(2):181–5.

505 10. Roche B, Aussel L, Ezraty B, Mandin P, Py B, Barras F. Iron/sulfur proteins biogenesis
506 in prokaryotes: formation, regulation and diversity. Biochim Biophys Acta. 2013
507 Mar;1827(3):455–69.

508 11. Lill R. Function and biogenesis of iron-sulphur proteins. Nature. 2009 Aug
509 13;460(7257):831–8.

510 12. Simon J, van Spanning RJM, Richardson DJ. The organisation of proton motive and
511 non-proton motive redox loops in prokaryotic respiratory systems. Biochim Biophys Acta.
512 2008 Dec;1777(12):1480–90.

513 13. Friedrich T, Dekovic DK, Burschel S. Assembly of the Escherichia coli
514 NADH:ubiquinone oxidoreductase (respiratory complex I). Biochim Biophys Acta. 2016
515 Mar;1857(3):214–23.

516 14. Lancaster CRD. Succinate:quinone oxidoreductases: an overview. Biochim Biophys
517 Acta. 2002 Jan 17;1553(1–2):1–6.

518 15. Davis BD. Mechanism of bactericidal action of aminoglycosides. Microbiol Rev. 1987
519 Sep;51(3):341–50.

520 16. Desnoyers G, Morissette A, Prévost K, Massé E. Small RNA-induced differential
521 degradation of the polycistronic mRNA iscRSUA. EMBO J. 2009 Jun 3;28(11):1551–61.

522 17. Massé E, Vanderpool CK, Gottesman S. Effect of RyhB small RNA on global iron use in
523 Escherichia coli. J Bacteriol. 2005 Oct;187(20):6962–71.

524 18. Massé E, Salvail H, Desnoyers G, Arguin M. Small RNAs controlling iron metabolism.
525 Curr Opin Microbiol. 2007 Apr;10(2):140–5.

526 19. Chareyre S, Mandin P. Bacterial Iron Homeostasis Regulation by sRNAs. Microbiol
527 Spectr. 2018 Mar;6(2).

528 20. Massé E, Gottesman S. A small RNA regulates the expression of genes involved in iron
529 metabolism in Escherichia coli. Proc Natl Acad Sci U S A. 2002 Apr 2;99(7):4620–5.

530 21. Seo SW, Kim D, Latif H, O'Brien EJ, Szubin R, Palsson BO. Deciphering Fur
531 transcriptional regulatory network highlights its complex role beyond iron metabolism in
532 *Escherichia coli*. Nat Commun. 2014 Sep 15;5:4910.

533 22. Giel JL, Nesbit AD, Mettert EL, Fleischhacker AS, Wanta BT, Kiley PJ. Regulation of
534 iron-sulphur cluster homeostasis through transcriptional control of the Isc pathway by [2Fe-
535 2S]-IscR in Escherichia coli. Mol Microbiol. 2013 Feb;87(3):478–92.

536 23. Mettert EL, Kiley PJ. Coordinate Regulation of the Suf and Isc Fe-S Cluster Biogenesis
537 Pathways by IscR Is Essential for Viability of Escherichia coli. J Bacteriol. 2014 Dec
538 15;196(24):4315–23.

539 24. Ezraty B, Barras F. The "liaisons dangereuses" between iron and antibiotics. FEMS
540 Microbiol Rev. 2016;40(3):418–35.

541 25. Mandin P, Chareyre S, Barras F. A Regulatory Circuit Composed of a Transcription
542 Factor, IscR, and a Regulatory RNA, RyhB, Controls Fe-S Cluster Delivery. mBio. 2016 20;7(5).

543 26. Massé E, Escorcia FE, Gottesman S. Coupled degradation of a small regulatory RNA
544 and its mRNA targets in Escherichia coli. Genes Dev. 2003 Oct 1;17(19):2374–83.

545 27. Kohanski MA, Dwyer DJ, Hayete B, Lawrence CA, Collins JJ. A common mechanism of
546 cellular death induced by bactericidal antibiotics. Cell. 2007 Sep 7;130(5):797–810.

547 28. Dwyer DJ, Kohanski MA, Collins JJ. Role of reactive oxygen species in antibiotic action
548 and resistance. Curr Opin Microbiol. 2009 Oct;12(5):482–9.

549 29. Unden G, Steinmetz PA, Degreif-Dünnwald P. The Aerobic and Anaerobic Respiratory
550 Chain of Escherichia coli and Salmonella enterica: Enzymes and Energetics. EcoSal Plus. 2014
551 May;6(1).

552 30. Desnoyers G, Massé E. Noncanonical repression of translation initiation through small
553 RNA recruitment of the RNA chaperone Hfq. Genes Dev. 2012 Apr 1;26(7):726–39.

554 31. Beauchene NA, Myers KS, Chung D, Park DM, Weisnicht AM, Keleş S, et al. Impact of
555 Anaerobiosis on Expression of the Iron-Responsive Fur and RyhB Regulons. mBio. 2015 Dec
556 15;6(6):e01947-01915.

557 32. Wang J, Rennie W, Liu C, Carmack CS, Prévost K, Caron M-P, et al. Identification of
558 bacterial sRNA regulatory targets using ribosome profiling. Nucleic Acids Res. 2015 Dec
559 2;43(21):10308–20.

560 33. Melamed S, Peer A, Faigenbaum-Romm R, Gatt YE, Reiss N, Bar A, et al. Global
561 Mapping of Small RNA-Target Interactions in Bacteria. Mol Cell. 2016 01;63(5):884–97.

562 34. Markham NR, Zuker M. UNAFold: software for nucleic acid folding and hybridization.
563 Methods Mol Biol Clifton NJ. 2008;453:3–31.

564 35. De Lay N, Schu DJ, Gottesman S. Bacterial small RNA-based negative regulation: Hfq
565 and its accomplices. J Biol Chem. 2013 Mar 22;288(12):7996–8003.

566 36. Lalaouna D, Eyraud A, Chabelskaya S, Felden B, Massé E. Regulatory RNAs Involved in
567 Bacterial Antibiotic Resistance. PLOS Pathog. 2014 Aug 28;10(8):e1004299.

568 37. Dersch P, Khan MA, Mühlen S, Görke B. Roles of Regulatory RNAs for Antibiotic
569 Resistance in Bacteria and Their Potential Value as Novel Drug Targets. Front Microbiol.
570 2017;8:803.

571 38. Felden B, Cattoir V. Bacterial Adaptation to Antibiotics through Regulatory RNAs.
572 Antimicrob Agents Chemother. 2018 May;62(5).

573 39. Kim T, Bak G, Lee J, Kim K-S. Systematic analysis of the role of bacterial Hfq-
574 interacting sRNAs in the response to antibiotics. J Antimicrob Chemother. 2015;70(6):1659–
575 68.

576 40. Zhang S, Liu S, Wu N, Yuan Y, Zhang W, Zhang Y. Small Non-coding RNA RyhB
577 Mediates Persistence to Multiple Antibiotics and Stresses in Uropathogenic Escherichia coli
578 by Reducing Cellular Metabolism. Front Microbiol [Internet]. 2018 Feb 6;9. Available from:
579 https://www.ncbi.nlm.nih.gov/pmc/articles/PMC5808207/

580 41. Lewis K. Persister cells: molecular mechanisms related to antibiotic tolerance. Handb
581 Exp Pharmacol. 2012;(211):121–33.

582 42. Murphy ER, Payne SM. RyhB, an iron-responsive small RNA molecule, regulates
583 Shigella dysenteriae virulence. Infect Immun. 2007 Jul;75(7):3470–7.

584 43. Deng Z, Meng X, Su S, Liu Z, Ji X, Zhang Y, et al. Two sRNA RyhB homologs from
585 Yersinia pestis biovar microtus expressed in vivo have differential Hfq-dependent stability.
586 Res Microbiol. 2012 Jul;163(6–7):413–8.

587 44. Kim JN, Kwon YM. Genetic and phenotypic characterization of the RyhB regulon in
588 Salmonella Typhimurium. Microbiol Res. 2013 Jan 15;168(1):41–9.

589 45. Unden G, Dünnwald P. The Aerobic and Anaerobic Respiratory Chain of Escherichia
590 coli and Salmonella enterica: Enzymes and Energetics. EcoSal Plus. 2008 Sep;3(1).

591 46. Parkhill J, Wren BW, Thomson NR, Titball RW, Holden MT, Prentice MB, et al.
592 Genome sequence of Yersinia pestis, the causative agent of plague. Nature. 2001 Oct
593 4;413(6855):523–7.

594 47. Salvail H, Caron M-P, Bélanger J, Massé E. Antagonistic functions between the RNA
595 chaperone Hfq and an sRNA regulate sensitivity to the antibiotic colicin. EMBO J. 2013 Oct
596 16;32(20):2764–78.

597 48. Broach WH, Egan N, Wing HJ, Payne SM, Murphy ER. VirF-independent regulation of
598 Shigella virB transcription is mediated by the small RNA RyhB. PloS One. 2012;7(6):e38592.

599 49. C. Manson J. Experiments with Gene Fusions. Edited by T. J. Silhavy, M. L. Berman and
600 L. W. Enquist. Published by Cold Spring Harbor Laboratory, Fulfillment Department, P.O. Box
601 100, Cold Spring Harbor, New York 11724, U.S.A. 1984. 350 pages. Paperback $40 ($48
602 outside U.S.). ISBN 0 87969 163 8. Genet Res - GENET RES. 1985 Apr 1;45.

603 50. Mandin P. Genetic screens to identify bacterial sRNA regulators. Methods Mol Biol
604 Clifton NJ. 2012;905:41–60.

605 51. Herisse M, Duverger Y, Martin-Verstraete I, Barras F, Ezraty B. Silver potentiates
606 aminoglycoside toxicity by enhancing their uptake. Mol Microbiol. 2017;105(1):115–26.

607 52. Seaver LC, Imlay JA. Are respiratory enzymes the primary sources of intracellular

608 hydrogen peroxide? J Biol Chem. 2004 Nov 19;279(47):48742–50.

609 53. Calhoun MW, Gennis RB. Demonstration of separate genetic loci encoding distinct

610 membrane-bound respiratory NADH dehydrogenases in Escherichia coli. J Bacteriol. 1993

611 May;175(10):3013–9.

612

Figure Legends

Figure 1. RyhB is involved in gentamicin resistance during iron starvation. A to D: strains were grown in LB (left panels) or in LB with DIP (250 μM) (right panels) for 3 h with or without the following antibiotics A: ampicillin (5 μg/mL); B: norfloxacin (25 ng / mL); C: tetracycline (5 μg/mL) and D: gentamicin (5 μg/mL). Colony forming units were counted to determine the number of surviving bacteria. Points were normalized relatively to t0 and plotted as $\log_{10}$ of surviving bacteria. The absolute c.f.u. at time-point zero was $\approx 5.10^7$ c.f.u. / mL for each sample. Error bars represent the standard deviations of three independent experiments. Statistical analysis were performed with Student's T-test: *$p < 0.05$; **$p < 0.01$; ***$p < 0.001$. E: WT (squares) and *ryhB* mutant (circles) strains were grown in LB (regular lines) or LB depleted for iron (dashed lines) with (red curves) or without (black curves) gentamicin. The number of c.f.u. was determined at different times. Error bars represent the standard deviations of three independent experiments. Statistical analysis were performed with Student's T—test: *$p < 0,05$; N.S.: Not significant.

Figure 2. RyhB induced gentamicin resistance is dependent on Nuo and Sdh. The *Δnuo Δsdh* (BEFB20) and *Δnuo Δsdh ΔryhB* (SC024) strains were grown for 3 h with or without gentamicin (5 μg / mL) in LB (left panels) or in LB with DIP 250 μM (right panels). Colony forming units were counted to determine the number of surviving bacteria. Points were normalized relatively to t0 and plotted as $\log_{10}$ of surviving bacteria. The absolute c.f.u. at time-point zero was $\approx 5.10^7$ c.f.u. / mL for each sample. Error bars represent the standard deviations of three independent

637 experiments. Statistical analysis were performed with Student's T-test: *p < 0,05;
638 **p < 0,01.
639
640 **Figure 3. RyhB decreases Nuo and Sdh enzymatic activities.** A: NADH specific
641 enzymatic activity of Nuo in WT or *ΔryhB* strain grown in LB (dark grey bars) or in LB
642 containing DIP (light grey bars) were determined by following the disappearance of
643 the D-NADH substrate by spectrophotometry (nmol / min / mg protein). B: Succinate
644 dehydrogenase activities in WT or *ΔryhB* strains grown in LB (dark grey bars) or in LB
645 containing DIP (light grey bars) were determined by following the absorbance of
646 DCPIP (nmol / min / mg protein). Bars represent the mean of at least three
647 experiments and error bars represent the standard deviations. Statistical analysis
648 were performed with Student's T-test: *p < 0,05; **p < 0,01; ***p < 0,001.
649
650 **Figure 4. RyhB represses *nuo* expression.** A: base-pairing predicted between
651 RyhB and *nuo* mRNA. Nucleotides belonging to *ryhB* are represented on top, those
652 corresponding to *nuo* on the bottom. Relative position to the transcriptional start site
653 of *ryhB* and *nuo* are indicated above and below the sequences, respectively. B: the
654 SC005 strain containing a P_{BAD}-*nuoA-lacZ* fusion was transformed with the empty the
655 plac vector or with the pRyhB plasmid containing *ryhB* under the control of an IPTG
656 inducible promoter. Cells were grown in LB containing ampicillin (25 μg/mL), IPTG
657 (100 μM) and arabinose (0,02 %) during 6 h after which ß-galactosidase activity was
658 determined. Specific activities are represented by arbitrary units that were empirically
659 determined to be approximately equivalent to Miller units. Error bars represent the
660 standard deviations of six independent experiments. C: strains containing the P_{BAD}-

661 *nuoA-lacZ* fusion, WT (SC005) or deleted for *ryhB* (SC006) were grown in LB with or
662 without DIP (200 μM) during 6h before ß-galactosidase activities were measured.
663 Each bar represents the mean from six independent experiments; error bars
664 represent the standard deviations. D: Strains containing either the P_{BAD}-*nuoA-lacZ* or
665 the P_{BAD}-$nuoA_{mut}$-*lacZ* fusions were transformed with the plac, pRyhB or pRyhBmut
666 plasmids and ß-galactosidase activity were determined. Each point represents the
667 mean from six or more experiments. E: WT and *ryhB* mutant cell extracts from
668 cultures grown in LB or in LB with DIP (250 μM) were subjected to immunoblot
669 analyses using antibodies raised against NuoG. Quantification represents the mean
670 of three different experiments.

671

672 **Figure 5. RyhB inhibits Nuo enzymatic activity by repressing *isc*.** Nuo (A) and
673 Sdh (B) specific enzymatic activities of *Δisc* and *Δsuf* mutants containing or not *ryhB*
674 grown in LB (dark grey bars) or in LB containing DIP (light grey bars) were
675 determined. Bars represent the mean of 3 independent experiments and error bars
676 represent the standard deviations. Statistical analysis were performed with Student's
677 T-test: *p < 0,05 ; **p < 0,01; ***p < 0,001; N.S.: Not significant.

678

679 **Figure 6. RyhB induces gentamicin resistance by inhibiting Fe-S clusters**
680 **maturation.** The *Δisc* (A) and the *Δsuf* (B) strains containing or not *ryhB* were grown
681 with (light grey bar) or without (dark grey bars) gentamicin (5 μg/mL) for 3 h in LB (left
682 panels) or in LB with DIP (250 μM) (right panels). After that, cells were diluted in PBS
683 and spotted on LB agar plates. c.f.u. and Log_{10} of surviving bacteria numbers were

684 determined. Error bars represent the standard deviation of three independent
685 experiments. Statistical analysis were performed with Student's T-test: *$p < 0,05$;
686 ***$p < 0,001$; N.S. : Not significant.

687

688 **Figure 7. Model for the RyhB induced resistance to gentamicin during iron**
689 **starvation.** When iron is not limiting (left panel), the Isc Fe-S biogenesis machinery
690 ensures the maturation of Nuo and Sdh, which generate a pmf that allows gentamicin
691 uptake. Gentamicin reaches the ribosome and incudes mistranslation, which renders
692 cells sensitive to the antibiotics. When iron is scarce (right panel), RyhB is expressed
693 and represses the expression of *nuo*, *sdh* and *isc.* The pmf is lowered and gentamicin
694 cannot enter the cytoplasm thus making cells resistant to the antibiotic.

695

Figure S1. RyhB increases the resistance to gentamicin during iron starvation. The WT and the *ΔryhB* mutant MIC were determined by growing cells in medium containing various concentrations of gentamicin and the iron chelator DIP (250 μM). The MIC was defined as the lowest drug concentration that exhibited complete inhibition of microbial growth

Figure S2. Sensitivity of *nuo* and *sdh* simple mutants to gentamicin. *Δnuo* (BEFB05), *Δnuo ΔryhB* (SC085), *Δsdh* (BEFB06) and *Δsdh ΔryhB* (SC086) strains were grown with or without gentamicin (5 μg / mL) for 3 h in LB with DIP 200 μM. Colony forming units were counted to determine the number of surviving bacteria. Points were normalized relatively to t0 and plotted as $\log_{10}$ of surviving bacteria. The absolute c.f.u. at time-point zero was ≈ 5.10^7 c.f.u. / mL for each sample. Error bars represent the standard deviation of three independent experiments. Statistical analysis were performed with Student's T-test: *p < 0,05 ; **p < 0,01 ; N.S. : Not significant

Figure S3. RyhB represses *sdh* expression. A: strain containing a P_{BAD}-*sdhC-lacZ* fusion (SC009) was transformed with the empty plac vector or with pRyhB plasmid containing *ryhB* under the control of an IPTG inducible promoter. Cells were grown in LB containing ampicillin (25 μg/mL), IPTG (100 μM) and arabinose (0,02 %) during 6 h after which ß-galactosidase activity was determined. Specific activities are represented by arbitrary units that were empirically determined to approximate Miller units. Error bars represent the standard deviations of six independent experiments. B: strains containing P_{BAD}-*sdhC-lacZ* WT (SC009) or deleted for *ryhB* (SC010) were

720 grown in LB with or without DIP (200 μM) during 6h before ß-galactosidase activities
721 were measured. Each bar represents the mean from six independent experiments. C:
722 WT and *ryhB* mutant cell extracts from cultures grown in LB or in LB with
723 DIP (250 μM) were subjected to Western blot analyses using antibodies raised
724 against SdhB. Quantification represents the mean of three different experiments.
725

726 **Figure S4. Gentamicin sensitivity can be directly correlated with Nuo and Sdh**
727 **specific activities.** Sensitivity to gentamicin of WT, *ΔryhB*, *Δisc*, *Δisc ΔryhB*, *Δsuf*
728 and *Δsuf ΔryhB* strains grown in LB (black points) or in LB containing DIP (red points)
729 were plotted relatively to their Nuo (A) or Sdh (B) enzymatic activity respectively. The
730 mean line represents linear correlation between the gentamicin sensitivity and
731 complexes activities A : $R^2 = 0{,}86593$; B : $R^2 = 0{,}77648$. Error bars represent the
732 standard deviation of three independent experiments.
733
734
735 **Table S1. Strains and plasmids used in this study.**
736
737 **Table S2. Oligonucleotides used in this study.**

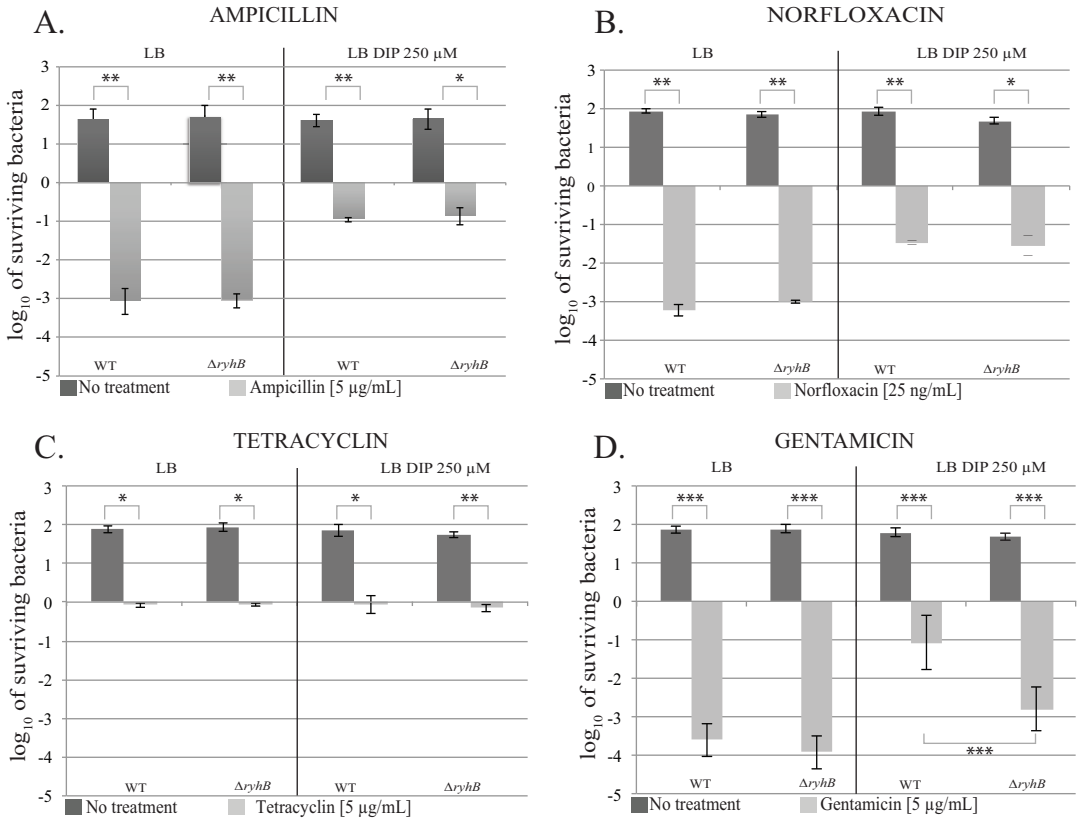

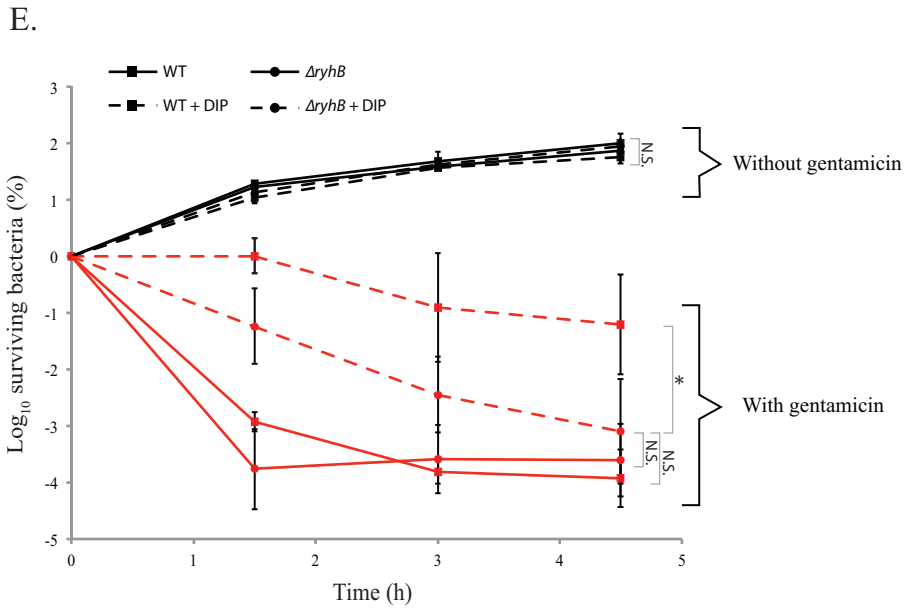

Figure 1.

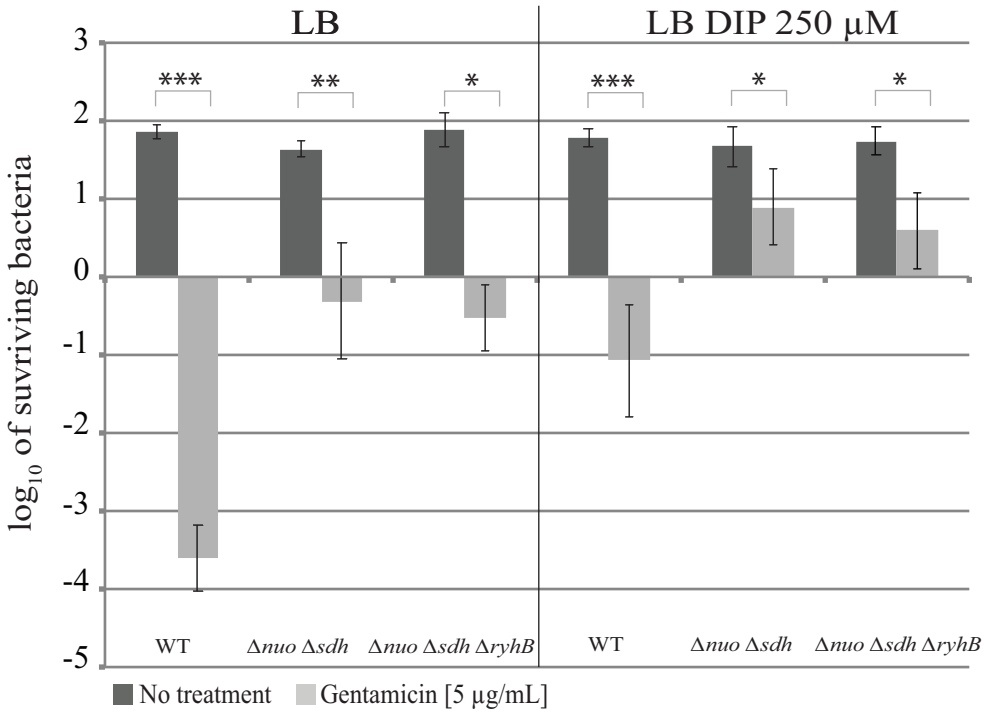

Figure 2.

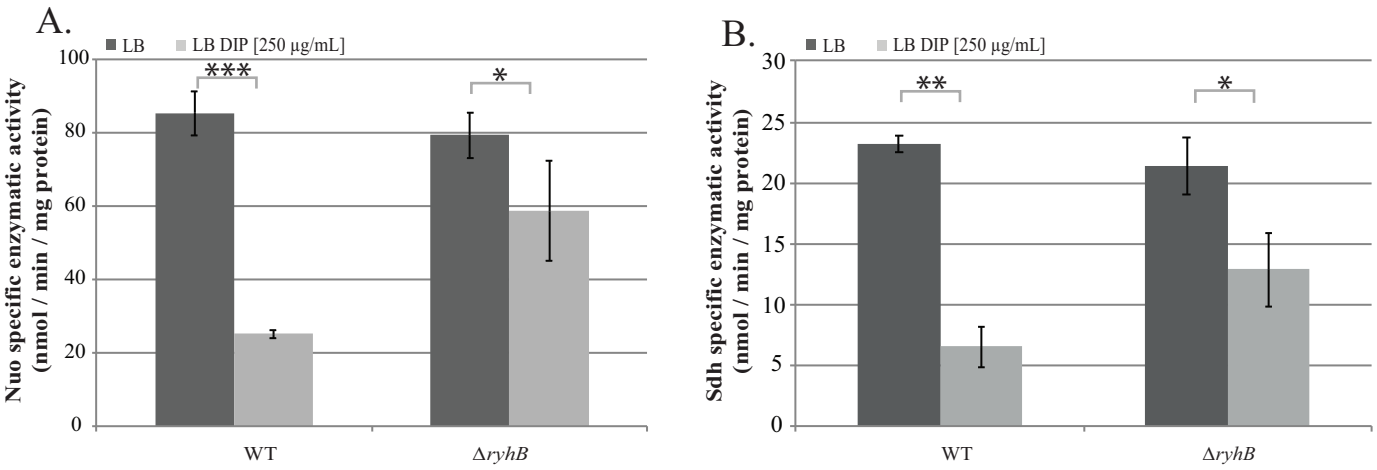

Figure 3.

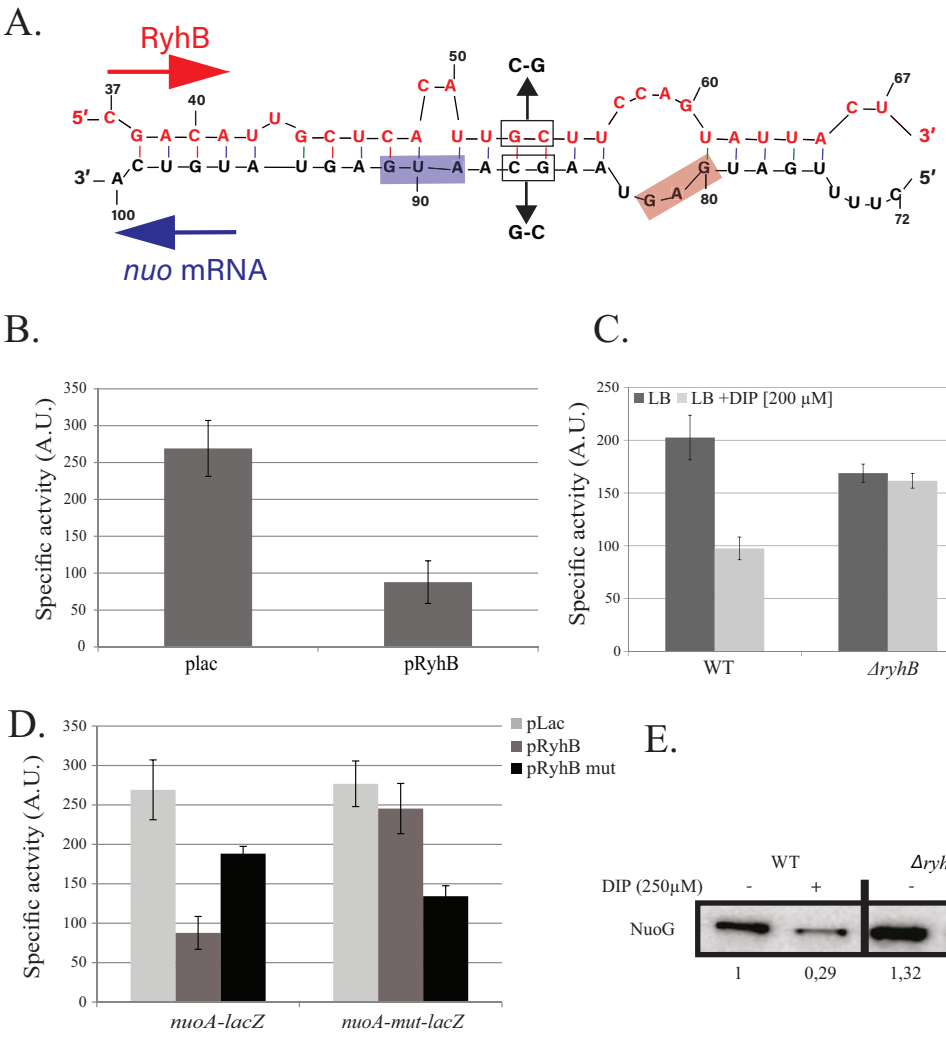

Figure 4.

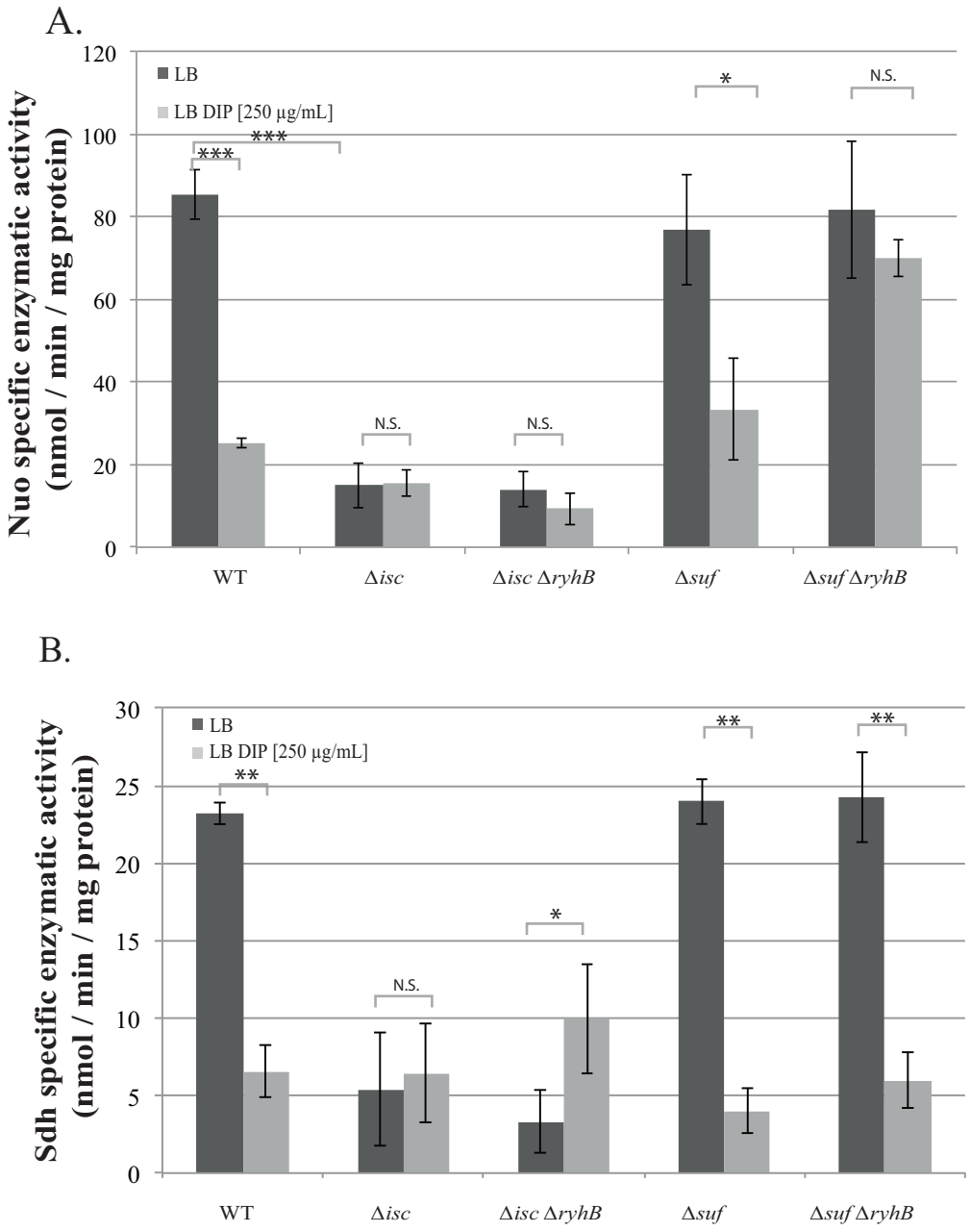

Figure 5.

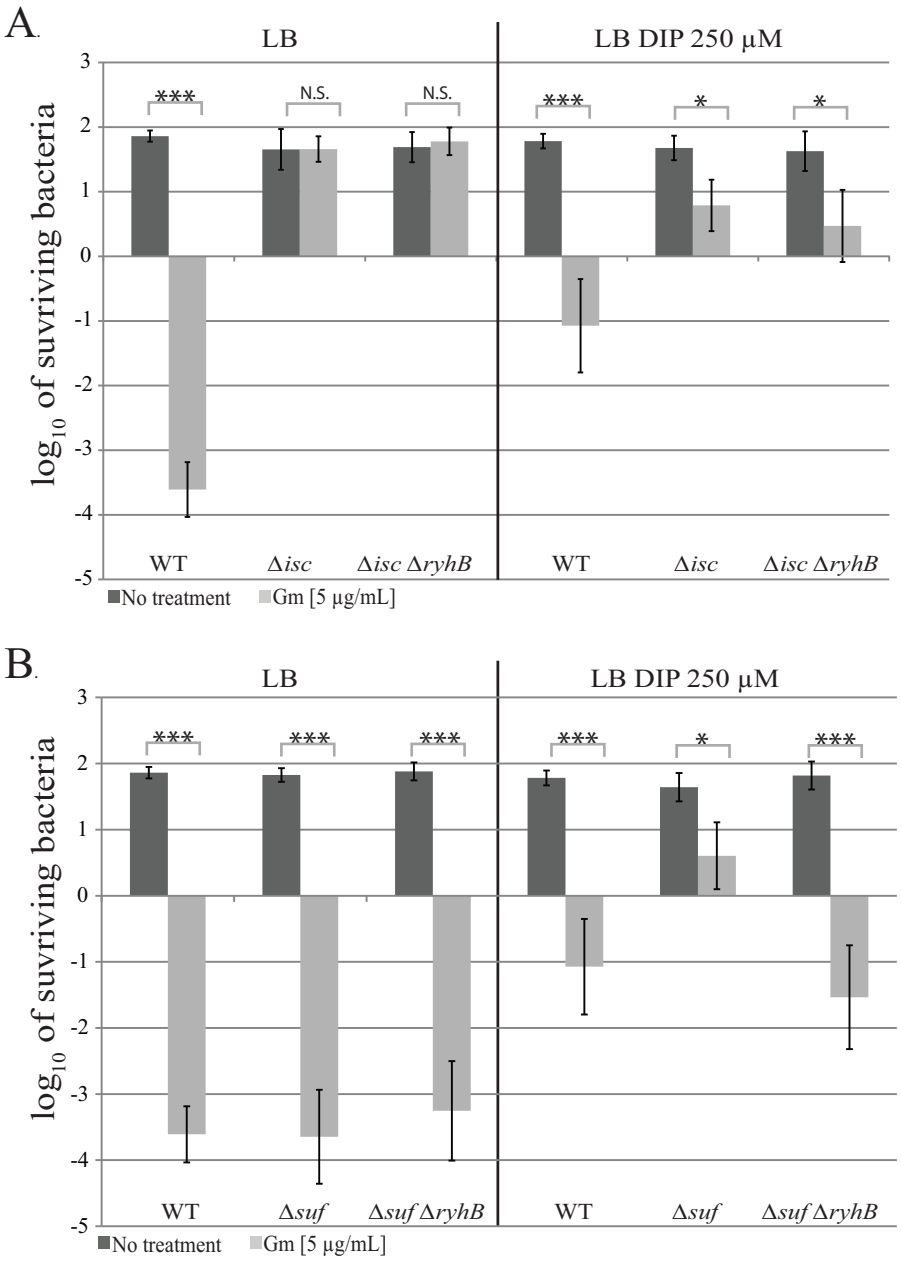

Figure 6.

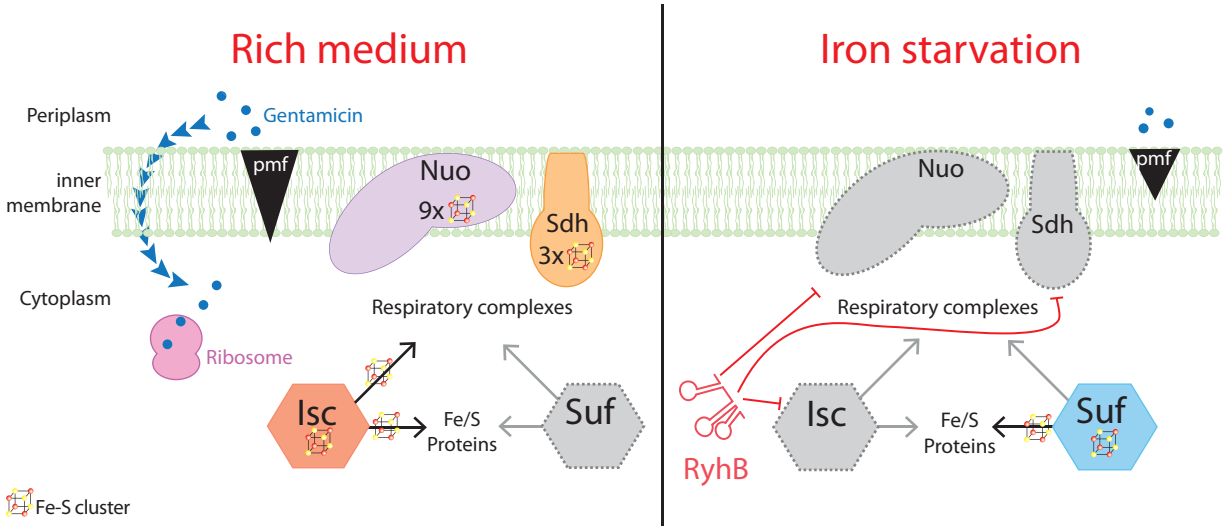

Figure 7.